

Supporting Information for

Electronic vs Structural Ordering in a Manganese(III) Spin Crossover Complex

Anthony J. Fitzpatrick,^a Elzbieta Trzop,^b Helge Müller-Bunz,^a Marinela M. Dîrțu,^c Yann Garcia,^c Eric Collet^{*b} and Grace G. Morgan^{*a}

^aSchool of Chemistry, University College Dublin, Belfield, Dublin 4, Ireland.

^bInstitut de Physique de Rennes, Université de Rennes 1 UMR UR1-CNRS 6251, 35000 Rennes, France.

^cInstitute of Condensed Matter and Nanosciences, Molecules, Solids and Reactivity (IMCN/MOST)
Université Catholique de Louvain, Place L. Pasteur 11348 Louvain-la-Neuve, Belgium.

1. Synthesis of [Mn(3,5-ClSal₂(323))]NTf₂, **1**
2. Magnetometry
3. Single Crystal X-ray Diffraction
4. Differential Scanning Calorimetry

1. Synthesis of [Mn(3,5-ClSal₂(323))]NTf₂, 1

To a well stirred solution of N,N-bis(aminopropyl)ethylenediamine (1 mmol, 0.183 mL) in 50:50 acetonitrile/ethanol (20 mL), 3,5-dichlorosalicylaldehyde (2 mmol, 0.382 g) was added, forming a yellow solution, this was allowed to stir for 15 min. Manganese(II) chloride hexahydrate (1 mmol, 0.198 g) was added to lithium bistrifluoromethanesulfonamide (1 mmol, 0.287 g) in 50:50 acetonitrile/ethanol (5-10 mL). The two solutions were then mixed and allowed to stir for one hour in air, yielding a dark brown solution of the Mn(III) complex resulting from aerial oxidation. Dark brown crystals of suitable quality for X-ray diffraction were formed upon slow evaporation of the solvent. Yield: 42%

Elemental: Theory: C, 33.78%, H, 2.83%, N, 8.21%, S, 7.52%

Found: C, 33.60%, H, 2.62%, N, 8.07%, S, 7.43%

Mass Spec: 573.20 (Found 573.00)

ATR-IR (cm⁻¹): 1586, 1452, 1364, 1227, 632

UV-Vis (MeCN):

λ/nm	$\epsilon/\text{Lmol}^{-1}\text{cm}^{-1}$
206	55529
238	42199
295	27545
385	9886

$[\text{MnL}_R]^+$ complexes:

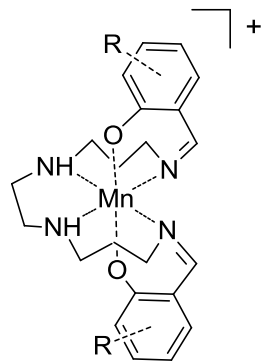


Fig. S1: Structure of the generic $[\text{MnL}_R]^+$ complex cation type.

2. Magnetometry

Variable temperature magnetic susceptibility data for a poly-crystalline sample of **1** was recorded on a Quantum Design MPMS[®] XL-7 SQUID magnetometer at 0.5 T in the range of 300 – 10 K in cooling and heating modes, Table S1. Corrections were made for the diamagnetic contributions of the sample using Pascal's constants and sample holder by measurement. Further scan rate measurements were performed in a field of 0.5 T at 10 K/min, 5 K/min, 2 K/min, 1 K/min and 0.5 K/min in settle mode, between 200 and 140 K in cooling and heating mode, Table S2. The $d\chi_M T/dT$ v T plot, Fig. S.2, clearly exhibits the effect of scan rate change.

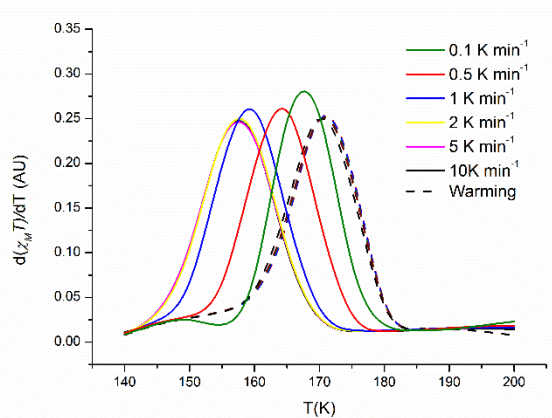


Fig. S.2: $d(\chi_M T)/dT$ v. T showing the shift in switching temperature with changing scan rate between INT and LT phases in complex **1** on cooling. No difference is observed in warming mode.

Table S1: $\chi_M T$ v T for full measurement of **1** at 5 K/min

Temperature (K)	$\chi_M T$ (cm ³ mol ⁻¹ K)	Temperature (K)	$\chi_M T$ (cm ³ mol ⁻¹ K)	Temperature (K)	$\chi_M T$ (cm ³ mol ⁻¹ K)	Temperature (K)	$\chi_M T$ (cm ³ mol ⁻¹ K)
300.0141	2.58744	154.9375	1.3094	10.00269	0.57395	150.0977	1.13095
294.8534	2.5699	149.9436	1.14156	10.00028	0.57452	155.095	1.16192
289.9244	2.5489	144.943	1.10656	14.99634	0.74223	160.0985	1.20013
284.9166	2.52725	139.9557	1.08375	19.9962	0.83247	165.1029	1.24541
279.9348	2.50682	134.9596	1.06592	25.00178	0.88306	170.1012	1.34744
274.9111	2.47764	129.9548	1.05137	29.99904	0.91366	175.1129	1.82113
269.9336	2.44979	124.9643	1.03726	35.00183	0.93358	180.1009	1.84115
264.8952	2.41948	119.965	1.03017	40.00142	0.94731	185.1099	1.85742
259.9242	2.38681	114.9673	1.02223	45.00188	0.95762	190.1006	1.87492
254.9124	2.35317	109.9698	1.01561	50.00795	0.96539	195.1149	1.89489
249.9238	2.31844	104.9789	1.01036	55.0125	0.97161	200.1063	1.91589
244.9211	2.28151	99.98084	1.00591	60.01585	0.97651	205.0993	1.93421
239.9171	2.2419	94.98401	1.00188	65.01937	0.981	210.1075	1.96517
234.9262	2.20003	89.99342	0.99847	70.02589	0.98512	215.1262	2.01717
229.9006	2.15525	84.99178	0.99475	75.03082	0.98882	220.1112	2.06813
224.9177	2.10839	80.01548	0.99101	80.03432	0.99142	225.1237	2.11871
219.9262	2.05958	75.00504	0.98796	85.03648	0.99599	230.1144	2.16391
214.9091	2.00761	70.00786	0.98347	90.04419	0.9996	235.1135	2.20789
209.9275	1.95589	65.00602	0.97471	95.05766	1.00342	240.1129	2.24952
204.9086	1.92658	60.01133	0.97422	100.0516	1.00763	245.11	2.28813
199.9135	1.90703	55.01149	0.96881	105.0625	1.01247	250.1138	2.32448
194.9269	1.88624	50.01209	0.96246	110.0645	1.01805	255.1168	2.35858
189.9164	1.86657	45.00492	0.95451	115.068	1.02468	260.1118	2.39068
184.9203	1.84894	40.00303	0.94419	120.0736	1.03218	265.1159	2.42047
179.9281	1.83294	34.99731	0.93002	125.0782	1.04121	270.1516	2.44896
174.9307	1.81864	30.00116	0.90955	130.0837	1.05255	275.1083	2.47646
169.9263	1.80361	24.9969	0.87858	135.0811	1.06571	280.1115	2.50395
164.9381	1.7839	20.0158	0.82776	140.0944	1.08343	285.1112	2.52648
159.9323	1.66534	15.00588	0.7378	145.0884	1.10538	290.1097	2.549
						295.1039	2.56997
						300.1059	2.59012

Table S2: Scan Rate Measurements of hysteretic loop

Temperature (K)	$\chi_M T$ ($\text{cm}^3 \text{mol}^{-1} \text{K}$)	Temperature (K)	$\chi_M T$ ($\text{cm}^3 \text{mol}^{-1} \text{K}$)	Temperature (K)	$\chi_M T$ ($\text{cm}^3 \text{mol}^{-1} \text{K}$)	Temperature (K)	$\chi_M T$ ($\text{cm}^3 \text{mol}^{-1} \text{K}$)	Temperature (K)	$\chi_M T$ ($\text{cm}^3 \text{mol}^{-1} \text{K}$)	Temperature (K)	$\chi_M T$ ($\text{cm}^3 \text{mol}^{-1} \text{K}$)
10 K/min		5 K/min		2 K/min		1 K/min		0.5 K/min		0.1 K/min	
200.0415	1.90109	200.0014	1.91096	199.9963	1.91411	199.995	1.91416	200.0205	1.91839	200.0026	1.91835
195.0082	1.88648	195.033	1.89374	195.0161	1.89672	195.0922	1.89744	195.025	1.90021	193.3728	1.89518
190.0298	1.87088	189.9788	1.87821	189.9971	1.87953	190.0889	1.88087	189.6136	1.88225	188.6662	1.8813
185.0386	1.85706	184.9941	1.86371	184.9908	1.86497	185.081	1.86598	184.6616	1.86852	183.5126	1.86806
180.0914	1.84438	180.0154	1.85061	180.0258	1.85233	180.0658	1.85288	180.0523	1.85591	178.5151	1.85502
175.0273	1.83291	175.0733	1.83741	174.9753	1.84026	175.0617	1.84052	174.7939	1.84367	173.5754	1.84366
170.0287	1.82144	170.025	1.82653	169.9875	1.82833	170.0708	1.82867	169.7779	1.83154	168.6171	1.74408
165.0298	1.80103	165.0358	1.80546	164.9884	1.80754	165.0711	1.7997	165.0409	1.58677	163.8788	1.25669
160.0252	1.64702	160.031	1.64601	159.9807	1.64715	160.0422	1.55794	159.8154	1.22487	153.4444	1.16902
155.0371	1.29062	155.0272	1.29718	154.9953	1.28667	155.0538	1.19931	154.8446	1.17217	155.002	1.18014
150.0509	1.13999	150.0259	1.14233	149.9782	1.14108	150.0401	1.13701	149.8443	1.14076	149.0546	1.14354
145.036	1.10945	145.0147	1.1087	144.9854	1.11063	145.0374	1.11138	145.002	1.11634	144.3407	1.1225
140.0475	1.09103	140.0277	1.09058	139.9886	1.0913	140.0444	1.0913	139.8803	1.09551	138.9159	1.10198
140.0065	1.08937	140.0115	1.08917	140.0015	1.09033	140.0096	1.09098	140.0084	1.09572	139.9984	1.10512
145.0567	1.10693	145.0487	1.10774	145.0314	1.10999	145.0127	1.11025	145.0007	1.11508	144.9973	1.12429
150.0501	1.13093	150.0565	1.13252	150.0323	1.13371	150.0066	1.13366	149.9959	1.13921	150.0009	1.1476
155.0516	1.16041	155.0462	1.16167	155.044	1.16407	155.0089	1.16333	154.9975	1.16924	154.9929	1.17755
160.0528	1.198	160.0544	1.19963	160.0333	1.20063	160.0098	1.20069	160	1.20706	159.9927	1.21459
165.0452	1.24894	165.0444	1.25165	165.034	1.25311	165.0099	1.25294	165.0004	1.25894	164.9995	1.2651
170.0167	1.45596	170.0598	1.43458	170.0341	1.43913	170.0112	1.45153	170.0029	1.46477	169.9956	1.50664
175.0598	1.83507	175.051	1.8377	175.0374	1.83903	175.0121	1.83896	175.0024	1.84488	174.9966	1.85331
180.0071	1.84722	180.0534	1.85056	180.0328	1.85147	180.0071	1.85105	180.002	1.85755	179.9989	1.86423
185.007	1.8616	185.0571	1.86397	185.0342	1.86474	185.0059	1.86414	184.9972	1.87104	185.0005	1.87854
190.0533	1.87706	190.0602	1.87912	190.0338	1.87964	190.0097	1.87961	190.0016	1.88554	189.9993	1.89386
195.0038	1.89244	195.0535	1.89581	195.0414	1.89644	195.0075	1.89608	195.0002	1.90261	194.9917	1.9099
200.0039	1.91121	200.06	1.91387	200.0383	1.91471	199.995	1.91407	200.0014	1.92097	199.9989	1.91769

3. Single Crystal X-ray Diffraction

Crystal data for **1** were collected at 120K, 185K, 210K and 260K using a Rigaku-Oxford Diffraction SuperNova diffractometer fitted with an EosS2 detector. All datasets were measured with Cu-K α radiation (1.54184 Å). The CrysAlisPro¹ software was used for data collection, cell constant determination and data reduction. Complete datasets were collected, assuming that the Friedel pairs are not equivalent. The structures were solved by direct methods using SHELXT² and refined by full matrix least-squares on F² for all data using SHELXL-97³. Hydrogen atoms were added at calculated positions and refined using a riding model. Anisotropic displacement parameters were used for all non-hydrogen atoms. Due to disorder of NTf₂ anion sites at each measured temperature, several geometric restraints (namely DFIX, DANG, and ISOR) and constraints (EADP) were applied in their model during the refinement process. The disorder of NTf₂ anion sites induces aperiodic modulation at 120K; due to weak satellite signal only average structure for 120K data is reported. To study changes of the unit cell parameters and volume, as well Bragg peaks intensity during the thermal phase transition of **1**, short temperature measurements, ~10min each, from 290K to 95K were performed during crystal cooling and/or heating with 2-5K temperature step.

Structures of **1** at 120 K (CCDC no. 1404709), 185 K (CCDC no. 1404711), 210 K (CCDC no. 1404710) and 260 K (CCDC no. 1428981) were deposited at the Cambridge Crystallographic Data Centre.

¹ CrysAlisPro, Rigaku-Oxford Diffraction Technologies (formerly Agilent Technologies), Version **1.171.37.35h**

² Sheldrick, G.M. (2015). Acta Cryst. A71, 3-8.

³ Sheldrick, G.M. (2008). Acta Cryst. A64, 112-122.

Table S3. Crystal data and structure refinement for **1**-120K.

Empirical formula	C24 H24 Cl4 F6 Mn N5 O6 S2	
Formula weight	853.34	
Temperature	120(2) K	
Wavelength	1.54184 Å	
Crystal system	Triclinic	
Space group	P-1	
Unit cell dimensions	a = 9.7733(3) Å	a = 101.301(2)°.
	b = 11.0266(4) Å	b = 100.490(2)°.
	c = 15.5654(3) Å	g = 101.672(3)°.
Volume	1567.37(8) Å ³	
Z	2	
Density (calculated)	1.808 Mg/m ³	
Absorption coefficient	8.594 mm ⁻¹	
F(000)	860	
Crystal size	0.2515 x 0.1661 x 0.0365 mm ³	
Theta range for data collection	4.219 to 71.100°.	
Index ranges	-11<=h<=11, -13<=k<=13, -19<=l<=13	
Reflections collected	20617	
Independent reflections	6014 [R(int) = 0.0294]	
Completeness to theta = 67.684°	99.9 %	
Absorption correction	Gaussian	
Max. and min. transmission	0.740 and 0.292	
Refinement method	Full-matrix least-squares on F ²	
Data / restraints / parameters	6014 / 78 / 546	
Goodness-of-fit on F ²	1.066	
Final R indices [I>2sigma(I)]	R1 = 0.0686, wR2 = 0.1849	
R indices (all data)	R1 = 0.0700, wR2 = 0.1864	
Largest diff. peak and hole	1.878 and -1.471 e.Å ⁻³	

Table S4. Crystal data and structure refinement for **1**-185K.

Empirical formula	C24 H24 Cl4 F6 Mn N5 O6 S2	
Formula weight	853.34	
Temperature	185.00(10) K	
Wavelength	1.54184 Å	
Crystal system	Triclinic	
Space group	P-1	
Unit cell dimensions	a = 9.9196(3) Å	a = 107.737(2)°.
	b = 20.8595(6) Å	b = 106.146(2)°.
	c = 16.9831(4) Å	g = 87.684(2)°.
Volume	3211.27(16) Å ³	
Z	4	
Density (calculated)	1.765 Mg/m ³	
Absorption coefficient	8.389 mm ⁻¹	
F(000)	1720	
Crystal size	0.2646 x 0.1465 x 0.0608 mm ³	
Theta range for data collection	4.116 to 71.315°.	
Index ranges	-12<=h<=12, -24<=k<=25, -20<=l<=15	
Reflections collected	28076	
Independent reflections	12282 [R(int) = 0.0454]	
Completeness to theta = 67.684°	99.7 %	
Absorption correction	Gaussian	
Max. and min. transmission	0.632 and 0.280	
Refinement method	Full-matrix least-squares on F ²	
Data / restraints / parameters	12282 / 145 / 1063	
Goodness-of-fit on F ²	1.047	
Final R indices [I>2sigma(I)]	R1 = 0.0433, wR2 = 0.1156	
R indices (all data)	R1 = 0.0493, wR2 = 0.1241	
Largest diff. peak and hole	0.632 and -0.645 e.Å ⁻³	

Table S5. Crystal data and structure refinement for **1**-210K.

Empirical formula	C24 H24 Cl4 F6 Mn N5 O6 S2	
Formula weight	853.34	
Temperature	210.00(10) K	
Wavelength	1.54184 Å	
Crystal system	Triclinic	
Space group	P-1	
Unit cell dimensions	a = 9.9211(4) Å	a = 102.260(4)°.
	b = 11.2426(5) Å	b = 100.491(4)°.
	c = 15.4284(7) Å	g = 100.192(4)°.
Volume	1611.34(12) Å ³	
Z	2	
Density (calculated)	1.759 Mg/m ³	
Absorption coefficient	8.360 mm ⁻¹	
F(000)	860	
Crystal size	0.2492 x 0.1683 x 0.0659 mm ³	
Theta range for data collection	4.129 to 71.340°.	
Index ranges	-12<=h<=12, -13<=k<=13, -18<=l<=16	
Reflections collected	14420	
Independent reflections	6168 [R(int) = 0.0263]	
Completeness to theta = 67.684°	99.8 %	
Absorption correction	Gaussian	
Max. and min. transmission	0.696 and 0.301	
Refinement method	Full-matrix least-squares on F ²	
Data / restraints / parameters	6168 / 40 / 544	
Goodness-of-fit on F ²	1.069	
Final R indices [I>2sigma(I)]	R1 = 0.0539, wR2 = 0.1489	
R indices (all data)	R1 = 0.0564, wR2 = 0.1517	
Largest diff. peak and hole	1.574 and -1.597 e.Å ⁻³	

Table S6. Crystal data and structure refinement for **1**-260K.

Empirical formula	C24 H24 Cl4 F6 Mn N5 O6 S2	
Formula weight	853.34	
Temperature	260(2) K	
Wavelength	1.54184 Å	
Crystal system	Triclinic	
Space group	P-1	
Unit cell dimensions	a = 9.9941(4) Å	a= 102.353(3)°.
	b = 11.2766(4) Å	b= 100.671(3)°.
	c = 15.4647(5) Å	g = 100.272(3)°.
Volume	1629.38(11) Å ³	
Z	2	
Density (calculated)	1.739 Mg/m ³	
Absorption coefficient	8.267 mm ⁻¹	
F(000)	860	
Crystal size	0.2423 x 0.1609 x 0.0601 mm ³	
Theta range for data collection	4.121 to 71.341°.	
Index ranges	-12<=h<=12, -13<=k<=13, -18<=l<=16	
Reflections collected	14653	
Independent reflections	6295 [R(int) = 0.0229]	
Completeness to theta = 67.684°	99.9 %	
Absorption correction	Gaussian	
Max. and min. transmission	0.682 and 0.298	
Refinement method	Full-matrix least-squares on F ²	
Data / restraints / parameters	6295 / 99 / 523	
Goodness-of-fit on F ²	1.105	
Final R indices [I>2sigma(I)]	R1 = 0.0708, wR2 = 0.2179	
R indices (all data)	R1 = 0.0744, wR2 = 0.2240	
Largest diff. peak and hole	1.535 and -1.356 e.Å ⁻³	

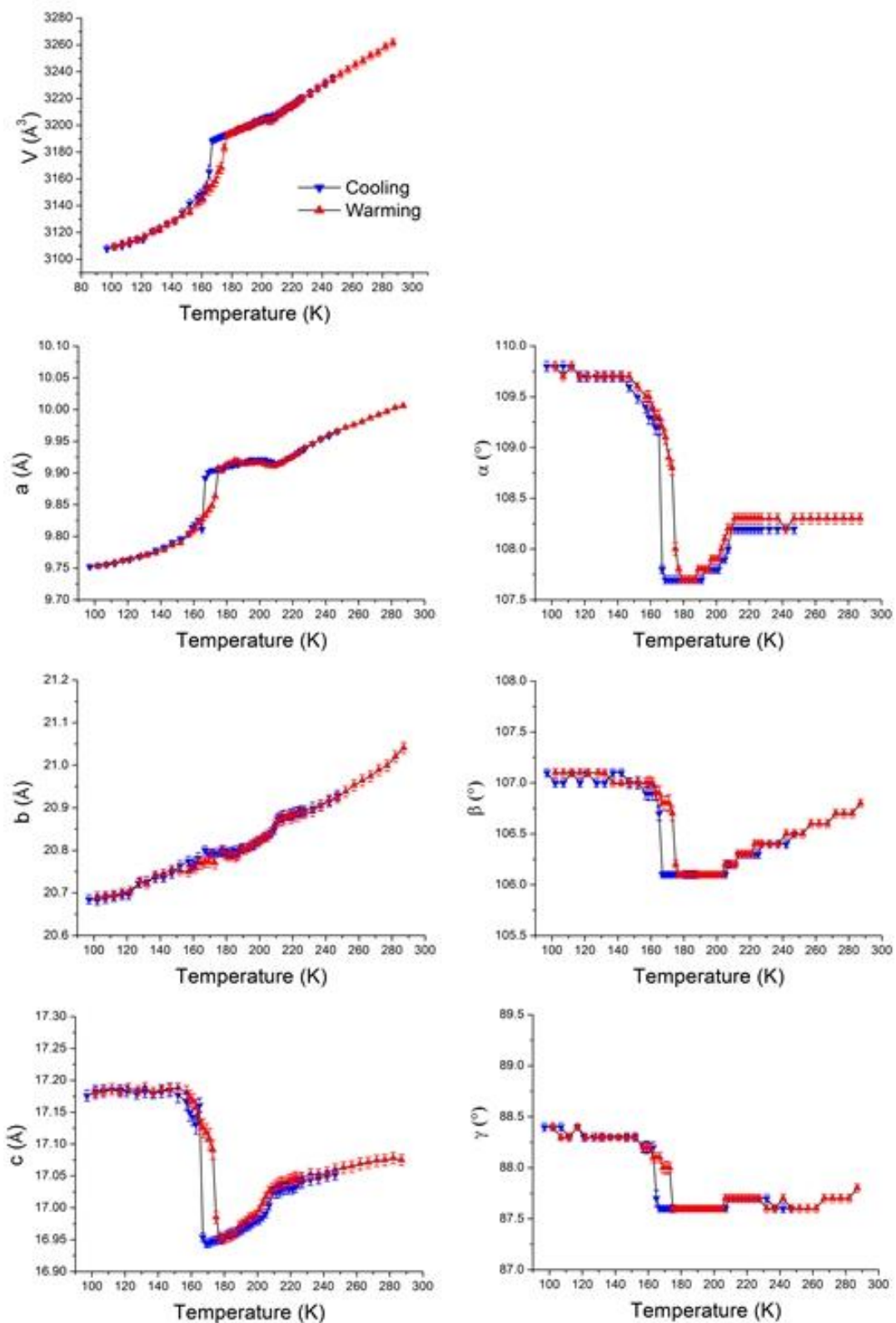


Figure S3: Change in function of temperature for the unit cell parameters and volume of complex **1** in the intermediate phase (INT) cell.

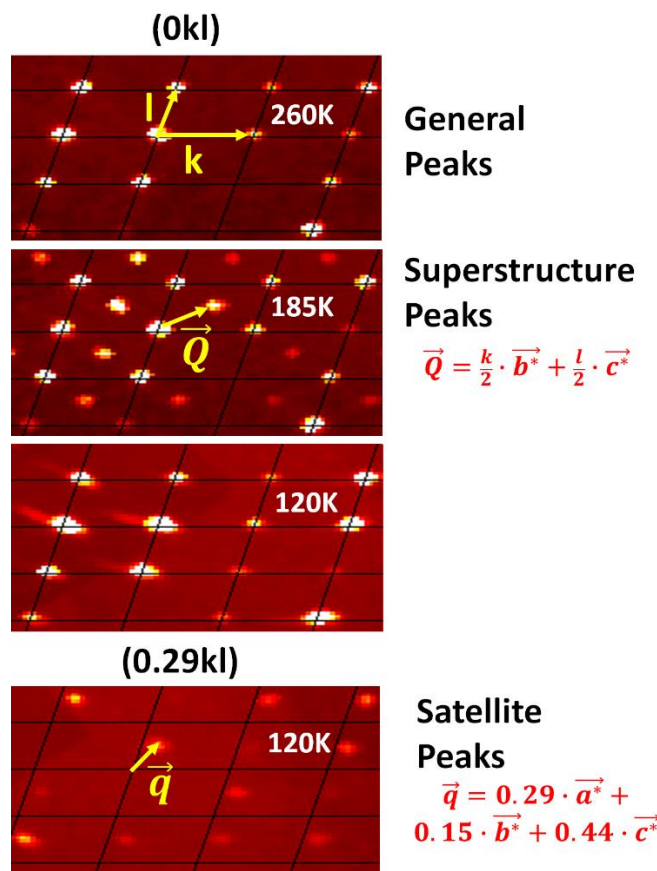


Figure S4: Reconstruction of $(0kl)$ reciprocal plane as function of temperature for complex 1 showing super lattice peaks for Intermediate Phase at \vec{Q} (185K) and satellite peaks for Low Temperature Phase at \vec{q} (120K).

4. Differential Scanning Calorimetry

DSC measurements were carried out in a He_(g) atmosphere using a Perkin-Elmer DSC Pyris 1 instrument equipped with a cryostat and operating down to 98 K. The purge gas was N2(g). Temperatures and enthalpies were calibrated over the temperature range 98–300 K using the solid/solid and liquid/solid transitions of pure cyclopentane (P99%, Acros).^[4] The calibration sample was introduced in an aluminum pan which was hermetically sealed using an encapsulating press. Calibration of the instrument was made at same scan rates which were used for the measurements of the sample. Next, aluminum capsules were loaded with 20–50 mg of sample and sealed. The energy data were converted to specific heat C_p (J/mol/K) using a PYRISTM DSC Software 7.0 module. The sample was maintained at room temperature for 5 min in order to allow the system to equilibrate, and was further cooled down from 300 to 105 K. The sample was maintained at 105 K for 5–10 min to reach equilibrium, followed by a similar scanning mode now on warming between 105 K and 300 K.

4. A. Rotaru, M. M. Dîrtu, C. Enachescu, R. Tanasa, J. Linares, A. Stancu, Y. Garcia, *Polyhedron* **2009**, 28, 2531–2536